Mol Neurobiol (2012) 46:487–494
DOI 10.1007/s12035-012-8312-7

Effect of Different Gentamicin Dose on the Plasticity of the Ribbon Synapses in Cochlear Inner Hair Cells of C57BL/6J Mice

Liping Chen · Siqing Xiong · Yi Liu · Xiuli Shang

Received: 6 May 2012 / Accepted: 13 July 2012 / Published online: 4 August 2012

Abstract Faithful information transfer at the hair cell afferent synapse requires synaptic transmission to be both reliable and temporally precise. The release of neurotransmitter must exhibit both rapid on and off kinetics to accurately follow acoustic stimuli with a periodicity of 1 ms or less. To ensure such remarkable temporal fidelity, the cochlear hair cell afferent synapse undoubtedly relies on unique cellular and molecular specializations. To study effects of different doses of gentamicin on the changes of synaptic ribbons of cochlear inner hair cells (IHCs) in mice, the availability of genetic information, transgenic and knock-out animals make the C57BL/6J mouse a primary model in biomedical research. Aminoglycoside ototoxicity, however, has rarely been studied in mature mice because they are considered highly resistant to the drugs. This study presents models for gentamicin ototoxicity in adult C57BL/6J mouse strains. Five-week-old mice were injected intraperitoneally once daily with 50–300 mg gentamicin base/kg body weight for 7 days. Higher doses of gentamicin appear to be associated with earlier hearing damage in C57BL/6J mice, although not necessarily with more severe damage. At 200 mg/kg, gentamicin appears to induce significant hearing damage while not significantly affect the animal's general condition. Therefore, 200 mg/kg may be an ideal dose for ototoxicity modeling in C57BL/6J mice using gentamicin. In the early period of different dose of gentamicin effect, when the number of hair cells had not changed, the number changes of IHC ribbon synapses had taken place. Through the number of ribbon synapses changing, IHCs increased or decreased connections with spiral ganglion nerves (SGNs). The ribbon synapses played a compensatory role for gentamicin ototoxicity, while this effect was not sufficient to maintain the normal threshold of hearing.

Keywords C57BL/6J mice · Aminoglycoside toxicity · Ribbon synapse · Hearing impairment

L. Chen · Y. Liu
Department of Neurology, The Ji'an Central People's Hospital,
106 Jing Gang Shan Road,
Ji'an City Jiangxi Province 343000, China

L. Chen · X. Shang (✉)
Department of Neurology, The First Affiliated Hospital of China Medical University, China Medical University,
92 North Second Road,
Shenyang 110001, China
e-mail: chenzijoycexiong@126.com

S. Xiong
Department of Urinary Surgery,
The Ji'an Central People's Hospital,
106 Jing Gang Shan Road,
Ji'an City Jiangxi Province 343000, China

Introduction

More than 60 years after their isolation and characterization, aminoglycoside (AG) antibiotics remain powerful agents in the treatment of severe gram-negative, enterococcal or mycobacterial infections [1, 2]. However, the clinical use of AGs is hampered by nephrotoxicity and ototoxicity, which often develop as a consequence of prolonged courses of therapy, or of administration of increased doses of these drugs. Increasing adoption of AGs poses the problem of toxicity directed to the kidneys and to the inner ear to scientists and physicians. In particular, AG-induced deafness can be profound and irreversible, especially in genetically predisposed patients. For this reason, an impressive amount of molecular strategies have been developed in the last decade to counteract the ototoxic effect of AGs.

In recent decades, people study of the ototoxic effect of AG antibiotics [1–5], but for hearing loss in mice, the research is still not deep enough. This includes both the types and modes of administration of the drug choosing, as well as the puzzle of the relationship between the dosages

of drug use and hearing loss. Ding Dalian, who used C57 mice to study the mechanism of deafness induced by, found that the outer hair cell cilia and cell body were obviously pathologically changed after AG antibiotics using, including the lack of cilia, cytoplasm and nucleus disintegration, etc. So he considered that the AG-induced deafness was closely related to the mechanism of these pathological changes [6]. It is little wonder that considerable attention has been paid to hair cell synapses in the cochlea and elsewhere. These efforts over the past decade have provided surprising insights into ribbon function, including the variable reliance on calcium influx at different synapses and the ability to spontaneously release multiple vesicles. Provocative as these findings are, our understanding of hair cell ribbon function remains far from complete. Fortunately the endpoint is certain—to explain the signalling of afferent neurons that is driven by transmitter release from the ribbon. Until now, guinea pigs and rats are the main choice of animal models in the research of AG-induced hearing damage. The main reason is that the bodies of these animals are relatively larger, the cochleae are much easily to get. But on the other hand, we should see that different factors leading to hearing loss tends to use mice [7–9], because the breeding and genetic characteristics of mice. They are more suitable for molecular biology research, the mechanism of genetic research and take genomics treatment to hearing damage [10, 11]. C57 mice are widely used in experiments. People have known that it is the animal model of presbycusis [12, 13]. Frisina, have used these mice for noise exposure study [14]. Actually, it is very important to study various types of deafness on one species of mice, because the results may allow us to know more clearly the difference between various types of deafness. Therefore, the observation of the inner hair cell afferent ribbon synapse of C57 mouse plays an important role for the molecular mechanism of in-depth study of hearing impairment. However, at present, only few studies use C57 mice to study the ototoxic effect of AGs [2, 15]. The reasons may be that some researchers worry that the presbycusis of C57 mice happened early which may affect the research. While, in previous studies of these mice, we found that, the time of hearing loss mostly happened after the birth of more than 6 months (20 weeks), so before that time C57 mice could be used as a drug-induced deafness research animal model. But which dose of medication for C57 mice will induce a typical deafness? And how the ribbon synapse changes? In order to answer these questions, we used C57BL/6J mice aged 5–6 weeks as our experimental animals, using different dosages of gentamicin exposure environment to induce sensorineural deafness. Then, we analysed the hearing data to get the most suitable drug-induced dose. Triple markers of immunohistochemical fluorescence with combination of the confocal microscope's serial scanning were used in our experiment, so as to explore the ribbon synaptic plasticity.

Material and Methods

Experimental Animals and Grouping

C57BL/6J mice with documented dates of birth were obtained from the Chinese Academy of Medical Sciences Animal Center (Beijing, China). All of the 90 mice (180 cochleae) were studied at 5 weeks of age. The animals were randomly divided into five groups (n=18), control group for the saline injection group (intraperitoneal injection of saline with the same volume of 300 mg/kg gentamicin group), the other four groups were intraperitoneally injected with different dosages (50, 100, 200, and 300 mg/kg) of gentamicin (Invitrogen, CA) once daily on the second (P2), fourth (P4), seventh (P7) days, auditory brainstem response (ABR) testing and the cochleae were processed. No outer or middle ear pathology was encountered in any of the animals studied and all procedures were executed in accordance with an animal protocol approved by the animal care and use committee and with the guide for the care and use of laboratory animals (NIH Publication No. 85-23, revised 1996).

Auditory-Evoked Brainstem Response (ABR) Analysis

ABR evaluations of hearing threshold in mice use method of Wu et al [1]. Mice were tested double blindly for ABR thresholds with equipment from Intelligent Hearing Systems (Miami, FL). The smart-EP v2.21 was used to generate specific acoustic stimuli and to amplify, measure, and display the evoked brainstem responses of anesthetized mice (concentration=0.45 mg/g body weight). Animals were kept warm with a heating pad in a soundproof shielded room during ABR recordings. Subdermal needle electrodes were inserted at the vertex and ventrolaterally to both ears of anesthetized mice. Specific auditory stimuli (broadband click and pure-tone pips of 4, 8, and16 kHz), with 20 beats/s recurrence rate, 1024 average superposition times, 20 min of scanning time, and 100–3,000 Hz of filtering wave bandwidth, were delivered binaurally through plastic tubes in the ear canals. Evoked brainstem responses were amplified and averaged and their wave patterns electronically displayed. Auditory thresholds were obtained for each stimulus by varying the sound pressure level (SPL) at 5-dB steps up and down in order to identify the lowest level at which an ABR pattern could be recognized. ABR thresholds were determined for each stimulus frequency by identifying the lowest intensity producing a reproducible ABR pattern on the computer screen (at least two consistent peaks).

Immunochemistry

After ABR tests, the mice of each dose groups were sacrificed by cervical dislocation, decapitation. Then the temporal bone was taken out and the cochlea was quickly separated. The round and oval windows were opened, and then perfusion was performed through them with 4 % paraformaldehyde overnight. The cochlea shell was separated from the basal turn under a dissecting microscope in 0.01 mmol/L PBS solutions, and then the parietal gyrus of the basilar membrane was separated and the vestibular membrane and the cover membrane were removed. The separated basilar membrane were washed three times in 0.01M PBS and preincubated for 30 min at room temperature in blocking solution of 5 % normal goat serum in 0.01M PBS with 0.3 %Trition X-100, then were incubated with combination of goat anti-mouse CtBP2 (E 16; C-terminal binding protein 2, C, end of combination of protein) antibody (1:200, SANTA CRUZ) and rabbit anti-mouse GluR 2&3 (glutamate or receptor 2/3 of AMPA receptor, the subunit 2/3, glutamate receptor subunit 2/3) antibody (1:200, SANTA CRUZ), left 4 °C overnight. The incubated samples were washed out in 0.01M PBS for three times and incubated in bovine anti-goat IgG FITC (fluorescein isothiocyanate; SANTA CRUZ) (1:100) room at 37 °C for 40 min, washed out three times again, then incubated in donkey anti-rabbit IgG-TR (markers of Texas the Red secondary antibody; SANTA CRUZ) (1:100) at 37 °C for 40 min, washed in PBS twice. Dropping a drop (approximately 40 μl) of DAPI (4′,6-diamidino-2-phenylindole; Santa Cruz) in the slide, basement membrane were tiled under a dissecting microscope, the coverslip covered the slide. The samples were imaged directly with fluorescent microscopy to test the specificity of the primary antibody.

Laser Scanning Confocal Microscope Imaging

The laser scanning confocal microscope was a Olympus FV1000 configuration (Japan) with 180× oil immersion objective. The excitation wavelength was 488 nm and 647 nm. Sequence scanning was performed in cochlear inner hair cells (IHCs) with an interval of 0.12 μm. Because immunohistochemical double-staining that performed with FITC and TR as the second antibodies, double-labeled fluoresce in color pairs showed orange (Fig. 1a–c). The sequence scanning started in the place where fluorescein color pairs appeared and stopped in the place where fluorescein color pairs disappeared. A two-dimensional image was collected. Sequence image of each group was put in a file and numbered in order. The sequence scanning for the parietal gyrus of 30 basilar membranes was performed. One visual field was selected from each basilar membrane for scanning, and 30 files were obtained.

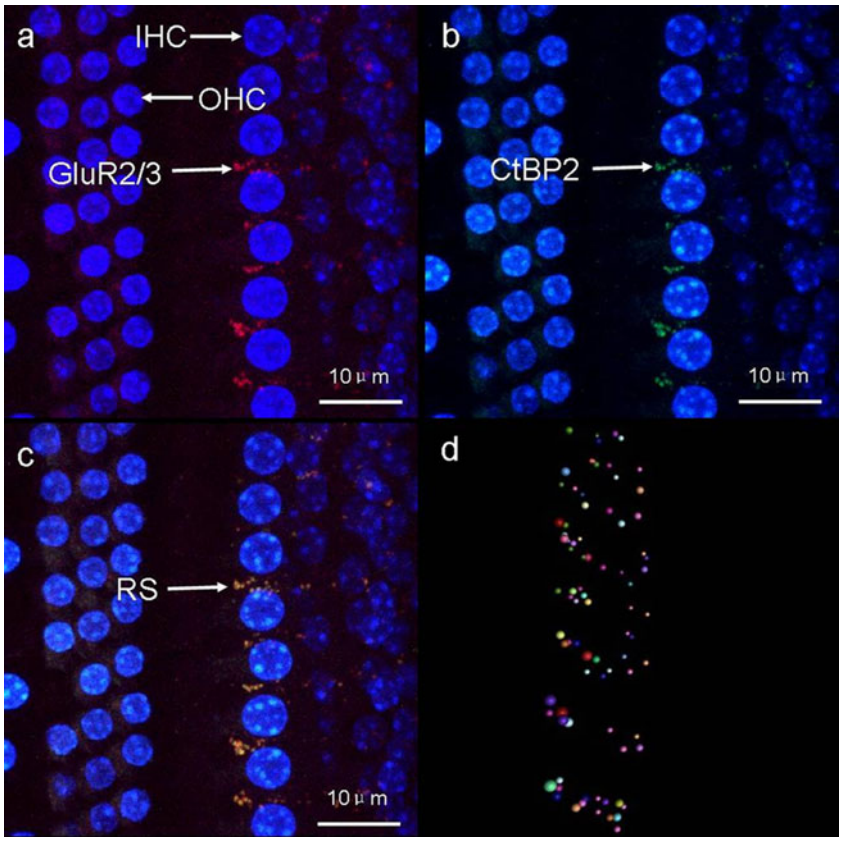

Fig. 1 The inner hair cell synapse. (a) Red fluorescence indicates TR labeled with GluR2/3 glutamate receptor subtypes and shows that the postsynaptic transmitter receptor clusters is labeled. (b) Green fluorescence indicates RIBEYE/CtBP2 labeled with FITC and shows that the presynaptic membrane is labeled. (c) Image synthetized by double channels. Orange fluorescence spots indicate the presence of a complete ribbon synapse. (d) Three-dimensional modeling for double immunofluorescent labeled fluorescence color pairs using 3DS MAX. Each marker indicates a fluorescein color pair, namely the presence of a ribbon synapse. (blue: contrast nuclear staining with DAPI)

Three-Dimensional Model Made with 3DS MAX

The collected two-dimensional images were put in the top view window of 3DS MAX in order to serve as the view port background. The first two-dimensional image was transferred, and a marker (shown in color ball) was made in the place where the orange fluorescence appeared, and then the next image was transferred. If the position where orange fluorescence appeared was the same as that in the previous image, the marker was not required, because it was considered to be the same synapse. If orange fluorescence appeared in other positions, which indicated a new synapse in this slice, a marker was made. Finally, the ribbon synapse number was obtained (Fig. 1d).

Statistical Analysis

All data are presented as mean ± SD. Statistical analysis for all the experiments was done by one way ANOVA Student–Newman–Keuls test, which was appropriate to determine significant differences between groups. P values of <0.05 were considered statistically significant differences.

Results

In this experiment, fluorescence positions were marked in each file, and two-dimensional image scanning and marking were performed in the 12 files. The repeat marked fluorescein color pairs were excluded. The best spatial distribution of fluorescein color pairs in 3DS MAX model was selected (Fig. 1d). Each marker in the figure indicated a complete ribbon synapse. The ribbon synapse number of IHCs in C57BL/6J is clearly and completely shown by double immunofluorescent labeling combined with 3DS three-dimensional modeling method, which provides feasibility for quantitative an analysis of the ribbon synapse number of IHCs. Our study showed higher doses of gentamicin appear to be associated with earlier hearing damage in C57BL/6J mice, although not necessarily with more severe damage. At 200 mg/kg, gentamicin appears to induce significant hearing damage while not significantly affecting the animal's general condition. The comparison of the hearing loss progression among the different dosage of gentamicin and the control group in Table 1. Therefore, 200 mg/kg may be an ideal dose for ototoxic modeling in C57BL/6J mice using gentamicin. In early period of different dose of gentamicin effect, when the number of hair cells had not changed, the number changes of IHC ribbon synapses had taken place (Table 2). Through the number of ribbon synapses changing, IHCs increased or decreased connections with spiral ganglion nerves (SGNs). The ribbon synapses played a compensatory role for gentamicin ototoxicity, while this effect was not sufficient to maintain the normal threshold of hearing.

Our results show that: (1) ABR thresholds on day 7 of treatment in the 50 mg/kg group (51.67±8.16 dB SPL, on day 4 in the 100 mg/kg group (48.89±9.16 dB SPL) and on day 2 in the 200- and 300-mg/kg groups (50.56±5.39 dB SPL and 50.50±6.85 dB SPL, respectively) were higher than prior to treatment (41.67±11.20 dB SPL, 40.83±10.07 dB SPL, 40.42±9.66 dB SPL and 40.00±11.0 dB

Table 1 Comparison of hearing loss progression in different dosages of gentamicin in C57BL/6J mice

Dose of drug (mg/kg)	Days of injection	Click(mean ± SD)	Mean ABR thresholds (dB SPL, mean ± SD		
			4 kHz	8 kHz	16 kHz
50	2	41.25±8.76	46.88±5.30	45.00±5.33	39.38±7.98
	4	42.50±10.8	48.33±5.16	47.50±5.45	40.00±6.90
	7	51.67±8.16	52.50±8.80	45.00±7.61	43.33±5.60
100	2	52.50±7.33	49.22±7.95	44.44±5.37	43.61±4.88
	4	48.89±9.16	54.44±8.73	45.00±5.56	47.22±5.76
	7	60.00±5.35	58.00±4.83	51.00±4.72	50.00±4.18
200	2	50.56±5.39	51.94±4.89	42.22±4.82	45.00±4.42
	4	58.50±8.83	59.00±5.68	50.50±6.79	49.00±6.16
	7	62.00±6.75	64.00±10.22	53.50±4.57	55.00±6.21
300	2	50.50±6.85	51.50±4.74	46.50±4.12	48.00±5.68
	4	46.67±7.53	57.50±8.80	45.83±7.56	44.17±7.41
	7	56.22±11.55	54.38±10.84	46.88±4.85	45.00±4.77
Control	2	43.00±8.23	48.00±5.37	40.50±6.77	37.00±6.14
	4	43.00±6.75	45.50±4.38	39.00±6.36	38.00±6.31
	7	48.00±6.75	47.00±4.22	43.00±4.34	37.50±6.42

Means of ABR thresholds (dB SPL) for each of the five groups for click, 4, 8, and 16 kHz stimuli

Table 2 Number of ribbon synapses per number of inner hair cell at each time point of each group

Dose of drug (mg/kg)	Days of injection		
	2	4	7
50	17.40±0.52	14.20±0.40	10.20±0.32
100	11.40±0.88	9.00±0.65	8.80±0.45
200	16.40±0.45	13.00±0.78	9.20±0.40
300	15.40±0.55	14.20±0.60	13.80±0.30
Control	16.20±0.24	15.90±0.46	16.00±0.21

SPL, respectively) ($P<0.05$). (2) ABR threshold shifts in different groups were as such: 200 mg/kg group >300 mg/kg group >100 mg/kg group >50 mg/kg group. (3) At high frequencies (8 kHz and 16 kHz) , ABR thresholds between the 50 mg/kg and 100 mg/kg groups were similar throughout the treatment period ($P>0.05$). ABR thresholds in the 100 mg/kg group increased sharply on days 4 and 7 of treatment ($P<0.05$), while the threshold in the 200 mg/kg group showed continuous increase from day 2 of treatment ($P<0.05$). ABR thresholds were at the highest level on day 7 of treatment in all groups. 200 mg/ kg dose caused the most obvious hearing damage, and hearing threshold gradually increased with the time going on. So this dosage may be the best dose of gentamicin that can induce obvious hearing damage on C57BL/6J mouse model. 2. In early period of gentamicin effect, when the number of hair cells had not changed, the number changes of IHC ribbon synapses had taken place (Table 2). (1) With the extension of the delivery time of each group, the number of ribbon synapses gradually reduced; (2) The number of ribbon synapses of the 100 mg /kg group were less than other dose groups at all time points; (3) Each number of ribbon synapses of 200 mg/kg and 300 mg/kg groups increased when compared with 100 mg/kg dose group, but still lower than the control group.

Discussion

AG antibiotics have been extensively used for the prophylaxis and the treatment of a wide variety of systemic infections, for the outstanding features displayed by these antibacterial agents, such as the concentration-dependent bactericidal activity, the post-antibiotic effect, the favorable pharmacokinetic profile, and the strong synergism with other antibiotics such as vancomycin and β-lactams [16]. The clinical use of AGs has always been hampered by nephrotoxicity and by the relatively highincidence of severe ototoxicity, which often develops as a consequence of prolonged courses of therapy, or after administration of increased doses of these agents. However, the emergence of severe, life-threatening, drug resistant infections has recently restored a new interest in AGs. Although hair cells in cristae, maculae or in the organ of Corti are the primary targets of AGs [17], an interesting study has demonstrated that cells in the stria vascularis, rich in mitochondria and responsible for the maintenance of the high potassium concentration of the endolymph (~157 mM, generating a positive 80–90 mV potential relative to the perilymph) [18], are targets of AGs like. It is now evident that outer hair cells are more sensitive to ototoxic injury than are inner hair cells. AGs are transported into hair cells, can be detected in perilymph 60–90 min after systemic administration, and remain detectable in hair cells up to 4 months after exposure. However, the role of inner hair cell ribbon synapses in the AG-induced hearing loss did not obtain enough attention and study.

Sensory synapses of the visual and auditory systems must faithfully encode a wide dynamic range of graded signals, and must be capable of sustained transmitter release over long periods of time [19]. Functionally and morphologically, these sensory synapses are unique: their active zones are specialized in several ways for sustained, rapid vesicle exocytosis, but their most striking feature is an organelle called the synaptic ribbon, which is a proteinaceous structure that extends into the cytoplasm at the active zone and tethers a large pool of releasable vesicles [20]. The function of synaptic ribbons depends on its composition. Progress has been made concerning the molecular identification of ribbon components and the understanding of the construction of synaptic ribbons.

A large number of studies have confirmed that the effectiveness of synaptic transmission is not fixed. Presynaptic neuronal excitability or neurotransmitter release may cause changes in postsynaptic potentials [21]. To complete the electrical signals pass, the synaptic function and form should change accordingly. This change can enhance or weaken synaptic transmission, by either increasing or reducing the number synapses: synaptic transmission performance changes are known as synaptic plasticity. Synaptic ribbons can vary even within a given type of ribbon synapse [21, 22]. Synaptic ribbons are dynamic structures, and the structural changes of ribbons appear to be either controlled by endogenous (circadian) signals or external signals, that is, changes in the surrounding illumination [19, 20]. In mouse retinas, changes in the surrounding illumination seem to regulate synaptic ribbon dynamics [20, 21]. In hair cells, even the shape of synaptic ribbons is associated with differences in functional properties. Differences in the Ca^{2+} dependency of exocytosis were observed in mature hair cells located either in high- or low-frequency regions of the organ of Corti, and these differences are correlated with synaptic ribbon morphology [22]. Hair cells in high-frequency regions appear to require larger surface ribbons. Hearing relies on faithful synaptic transmission at the ribbon synapse of IHCs. At present, the function of presynaptic ribbons at these synapses is still largely unknown. As to our results, the

reasons may be as follows: (1) from the view of ribbon synapse genetic point, the major structural protein of the RS—the RIBEYE protein synthesis reduced after small doses of gentamicin (50, 100 mg/kg) being applied. While the mRNA stored in the inner hair cells increased in the stimulation of large dose of gentamicin (200, 300 mg/kg). Then the synaptic protein synthesis raised, leading to the expression of the synapse itself partially restored, that enhanced vesicle fusion and synaptic transmitter release in inner hair cell ribbon synapse. It strengthened the neural connections between the inner hair cells and spiral ganglion neuron. It played a certain compensatory role to the ototoxicity of gentamicin eventually. However, the ribbon synapses of this change did not play the role of fully compensatory to the ototoxicity due to the increased ABR threshold. (2) The presynaptic synapse release neurotransmitter of glutamate, which is mainly mediated fast excitatory synaptic transmission in the central nervous system (CNS). Studies have shown that glutamate plays a vital role in CNS signal transmission, neural development and synaptic plasticity (including memory, learning). But large number of glutamate could be neurovirulent, namely excitotoxicity. Therefore, the increase or decrease of synaptic expression would affect the signal transmission. When given high dose of gentamicin, a large number of glutamate released, while the ability of glutamate uptake in postsynaptic membrane descended. So, glutamate could not be completely recycled, resulting in a large number of glutamate accumulation which produced excitotoxicity. This change could cause neurons to be lethal, while excitotoxicity in CNS. The distance between the hair cell and spiral ganglion cells is far away from the ganglion cells, it may aggravate the excitotoxicity limited to the surrounding acoustic nerve that with no myelin sheath. As dose increased, excitotoxicity enhanced, inducing synapse that around ganglion cells to swell, crack, shrink, leading to the occurrence of deafness eventually. On the other hand, when large dose applicated, the body might restore expression of the ribbon synapse through the negative feedback regulation mechanism, while the compensatory role was not enough. The result is hearing loss. However, to know the precise morphology, structure and function of synapse, technical means of immune markers, electron microscopy, protein quantitative analysis, and neural electrophysiology (patch clamp), etc. should be used in the future. Only in this way can we reveal the comprehensive characteristics of synaptic plasticity of inner hair cells.

The conclusion of our study may differ from some studies before, for example, many studies showed that hearing deficit was dose-dependent. This difference may be due to the use of different types of animals [23], and different type of drugs [3]. There have been reported that hearing loss of mice was dose-dependent when use of kanamycin [24]. But we are not clear whether this difference was related to the different administration of drug. Our studies showed another kind of hearing loss characteristic: the time of the hearing threshold increased occurred in advance, rather than increased in degree. It seems that there is an upper limit of hearing damage indicated by gentamicin in C57BL/6J mice. We speculate that perhaps in the cochlea, there is an accumulated capacity to carry gentamicin and its toxic effects. So redundant capacity of the drugs is difficult to enter the cochlea, but do poison to heart and kidneys. Large doses of gentamicin can directly lead to the death of the animal. In our previous study, more than half of the mice were killed when 400 mg/kg dose was administrated. While there was no significant difference between the mice those still alive and other groups of mice in hearing threshold. Comparison the hearing loss of 300 mg/kg group and 200 mg/kg group, the latter increased in both click and tone burst (4, 8, 16 kHz). In contrast, 300 mg/kg group did not show such uniform characteristics. In addition, Comparison of 200 mg/kg group, 100 mg/kg group and 50 mg/kg group, we can find that hearing threshold of 200 mg/kg group did not only increase significantly at each frequency, but also had equilibrium distribution. Therefore, the use of 200 mg/kg of gentamicin in C57BL/6J mice can induce significant hearing damage, the frequency distribution is balanced and it is security.

There are many researches in the mechanism of gentamicin hearing damage in mice, results mainly related to the damage of the cilia and outer hair cells, then causes hearing decline [5, 15, 25]. Some previous studies showed that afferent ribbon synapse of inner hair cells may be another site where AG antibiotics damaged [15]. Synaptic ribbons (also called synaptic bodies or dense bodies) are the name-giving presynaptic specializations of ribbon synapses and have been known since the early days of electron microscopy [19]. Although diverse in shape, they have distinct features in common. Synaptic ribbons are electron-dense structures of considerable size. They are surrounded and physically in touch with a large amount of synaptic vesicles which are positioned by the ribbon in close proximity to the presynaptic neurotransmitter release site, the active zones. Synaptic ribbons can vary even within a given type of ribbon synapse. Synaptic ribbons are dynamic structures, and the structural changes of ribbons appear to be either controlled by endogenous (circadian) signals or external signals, that is, changes in the surrounding illumination [19, 20]. In mouse retinas, changes in the surrounding illumination seem to regulate synaptic ribbon dynamics [20, 21]. There is a correlation between the number of synaptic ribbons and functional properties of the synapse. The removal of material from the synaptic ribbon, for example, from rod synaptic ribbons during lightness, is mediated by the dissociation of spherical synaptic ribbons (synaptic spheres) from the bar-shaped ribbons.

Synaptic spheres are also suggested to be precursors in the assembly of bar-shaped synaptic ribbons [21, 26]. A modular assembly of synaptic ribbons has been proposed in which synaptic ribbons assemble from RIBEYE subunits [27]. The modular assembly hypothesis of synaptic ribbons from individual RIBEYE subunits provides also an explanation for the assembly of synaptic ribbons from smaller RIBEYE subunits. The assembly of synaptic ribbons from RIBEYE subunits likely is a multistep process which also includes the synaptic spheres, spherical synaptic ribbon-like structures. CtBP1 is related to the B-domain of RIBEYE and a component of synaptic ribbons [28]. The function of CtBP1 in synaptic ribbons is not yet clear. CtBP1 and CtBP2/RIBEYE (B)-domain bind to the cytomatrix protein bassoon which is found at the active zone of ribbon synapses [28, 29]. The anti-CtBP2 antibody may specifically link with domain B of RIBEYE to specifically label presynaptic membranes. Glutamate receptor 2&3 (GluR 2&3) exists widely in postsynaptic membranes. Therefore, CtBP2 and GluR 2&3 are simultaneously labeled, green fluorescence indicates CtBP2 (showing RIBEYE presence) and red fluorescence indicates GluR 2&3 presence. If two-channel scanning is carried out, the site where red and green fluorescence simultaneously occurs will show orange which indicates the presence of a complete ribbon synapse. The 3DS MAX software package served as the basic software of three-dimensional modeling possesses strong capabilities for three-dimensional reconstruction and analog computation. The software may be used not only to study the spatial distribution of objects, but also to investigate their morphology and volume, which establishes a basis for quantitative analysis [30, 31]. In 3DS MAX, the two-dimensional images were part of the background, and fluorescein color pairs were marked (shown in color ball). At first, the first two-dimensional image was transferred, and a marker was made in the place where orange fluorescence appeared, and then the next image was transferred. If the position where orange fluorescence appeared was the same as that in previous image, the marker did not need to be done. If orange fluorescence appeared in other positions, a marker was made, which avoided making repeated markers for the same synapse. We selected three time points (2, 4, and 7 days) to study the change in the number of ribbon synapses after intraperitoneal injection of different doses of gentamicin, so as to observe the relationship of hearing loss and changes in the number of ribbon synapses.

This study established a stable model of gentamicin ototoxicity in mice. We can not only study the synaptic mechanisms and treatment, but also observe the role of deafness genes, related proteins and other factors in this model. Inner hair cell ribbon synapse play a very important role in signal transmission between hair cells and spiral ganglion neuron. By study the number and function of IHC ribbon synapse, we added a new aspect of pathogenesis induced by gentamicin ototoxicity in C57BL/6 J mice. It laid a good foundation for the pathological study of synapses derived from other causes of hearing impairment. Although we know a great deal about ribbon synapses, mysteries still abound. The multidisciplinary approach to the hair cell ribbon synapse has for the first time quantitatively described important aspects of the synapse's structure and function. Most importantly, despite all limiting uncertainty, we begin to relate molecules, structure and function. Although still debated, the concept of a readily releasable pool has been substantiated for the ribbon synapse of several hair cells. We have gained a few insights into the mechanisms underlying the incredible temporal precision of synapses that participate in the coding of sound. However, we are far from a comprehensive molecularly defined model of ribbon structure and function. New approaches are needed to understand them—such as high-resolution optical imaging in living cells or ultrastructural methods to catch the vesicles in the act, and ways to alter ribbon function in real time during electrophysiological experiments. Ear-specific genetic deletion also will be helpful to investigate synaptic protein function in hair cell sound coding. A more precise and direct biophysical analysis of single hair cell synapses will require combined pre- and postsynaptic recordings as well as optical measurements, such as evanescent wave microscopy and confocal techniques. The optical approach will be strongly facilitated by the generation of genetically targeted fluorescent vesicle tags. It should also be kept in mind that not all ribbons may operate in the same way and, as studies advance, it will be important to discriminate between general features and unique specializations. After all, ribbons vary enormously in size and postsynaptic architecture, and so the relative importance of fast synchronous release versus slow sustained release is likely to vary as well, depending on cell type and on the functional context of the synapse. In this regard, ribbon synapses are no different from conventional synapses, which also vary widely in their functional properties.

Acknowledgments This work was supported by Education Fund L2010564, Technology Fund 2011225020 and Doctoral Scientific Research Fund 20101142 of Liaoning Province of China; National Natural Science Found 81100243.

References

1. Wu WJ, Sha SH, McLaren JD, Kawamoto K, Raphael Y, Schacht J (2001) Aminoglycoside ototoxicity in adult CBA, C57BL and BALB mice and the Sprague Dawley rat. Hear Res 158:165–178

2. Nakagawa T, Yamane H, Shibata S, Nakai Y (1997) Gentamicin ototoxicity induced apoptosis of the vestibular hair cells of guinea pigs. Eur Arch Otorhinolaryngol 254:9–14
3. Murillo-Cuesta S, Contreras J, Cediel R, Varela-Nieto I (2010) Comparison of different aminoglycoside antibiotic treatments to refine ototoxicity studies in adult mice. Lab Anim 44:124–131
4. Rizzi MD, Hirose K (2007) Aminoglycoside ototoxicity. Curr Opin Otolaryngol Head Neck Surg 15:352–357
5. Lin CT, Young YH, Cheng PW, Lue JH (2010) Effects of gentamicin on guinea pig vestibular ganglion function and on substance P and neuropeptide Y. J Chem Neuroanat 40:286–292
6. Dehne N, Rauen U, de Groot H, Lautermann J (2002) Involvement of the mitochondrial permeability transition in gentamicin ototoxicity. Hear Res 169:47–55
7. Gooi A, Hochman J, Wellman M, Blakeley L, Blakley BW (2008) Ototoxic effects of single-dose versus 19-day daily-dose gentamicin. J Otolaryngol Head Neck Surg 37:664–667
8. Lee JE, Nakagawa T, Kim TS, Iquchi F, Endo T, Kita T, Murai N, Natio Y, Lee SH, Ito J (2004) Signaling pathway for apoptosis of veshair cells of mice due to aminoglycosides. Acta Otolaryngol Suppl 551:69–74
9. Castillo E, Carricondo F, Bartolomé MV, Vicente-Torres A, Poch Broto J, Gil-Loyzaqa P (2006) Presbycusis: neural degeneration and aging on the auditory receptor of C57/BL6J mice. Acta Otorrinolaringol Esp 57:383–387
10. Brown SD, Hardisty-Hughes RE, Mburu P (2008) Quiet as a mouse: dissecting the molecular and genetic basis of hearing. Nat Rev Genet 9:277–290
11. Pfannenstiel SL, Praetorius M, Plinkert PK, Brouqh DE, Staecker H (2009) Bcl-2 gene therapy prevents aminoglycoside-induced degeneration of auditory and vestibular hair cells. Audiol Neurootol 14:254–266
12. Idrizbegovic E, Bogdanovic N, Willott JF, Canlon B (2004) Age-related increases in calcium-binding protein immunoreactivity in the cochlear nucleus of hearing impaired C57BL/6J mice. Neurobiol Aging 25:1085–1093
13. McFadden SL, Ding D, Salvi R (2001) Anatomical, metabolic and genetic aspects of age-related hearing loss in mice. Audiology 40:313–321
14. Frisina RD, Newman SR, Zhu X (2007) Auditory efferent activation in CBA mice exceeds that of C57s for varying levels of noise. J Acoust Soc Am 121:29–34
15. Maudonnet EN, de Oliveira JA, Rossato M, Hyppolito MA (2008) Gentamicin attenuates gentamicin-induced ototoxicity-self-protection. Drug Chem Toxicol 31:11–25
16. Vakulenko SB, Mobashery S (2003) Versatility of aminoglycosides and prospects for their future. Clin Microbiol Rev 16:430–450
17. Forge A, Schacht J (2000) Aminoglycoside antibiotics. Audiol Neurootol 5:3–22
18. Takeuchi S, Ando M, Kakigi A (2000) Mechanism generating endocochlear potential: role played by intermediate cells in stria vascularis. Biophys J 79:2572–2582
19. Wagner HJ (1997) Presynaptic bodies ("ribbons"): from ultrastructural observations to molecular perspectives. Cell Tiss Res 287:435–446
20. Vollrath L, Spiwoks-Becker I (1996) Plasticity of retinal ribbon synapses. Microsc Res Tech 35:472–487
21. Spiwoks-Becker I, Glas M, Lasarzik I, Vollrath L (2004) Mouse photoreceptor synaptic ribbons lose and regain material in response to illumination. Eur J Neurosci 19:1559–1571
22. Johnson SL, Forge A, Knipper M, Münkner S, Marcotti W (2008) Tonotopic variation in the calcium dependence of neurotransmitter release and vesicle pool replenishment at mammalian auditory ribbon synapses. J Neurosci 28:7670–7678
23. Roux I, Safieddine S, Nouvian R, Grati M, Simmler MC, Bahloul A, Perfettini I, Le Gall M, Rostaing P, Hamard G, Triller A, Avan P, Moser T, Petit C (2006) Otoferlin, defective in a human deafness form, is essential for exocytosis at the auditory ribbon synapse. Cell 127:277–289
24. Meyer AC, Frank T, Khimich D, Hoch G, Riedel D, Chapochnikov NM, Yarin YM, Harke B, Hell SW, Eqner A, Moser T (2009) Tuning of synapse number, structure and function in the cochlea. Nat Neurosci 12:444–453
25. Bertolaso L, Bindini D, Previati M, Falgione D, Lanzoni I, Parmeggiani A, Vitali C, Corbacella E, Capitani S, Martini A (2003) Gentamicin-induced cytotoxicity involves protein kinase C activation, glutathione extrusion and malondialdehyde production in an immortalized cell line from the organ of corti. Audiol Neurootol 8:38–48
26. Regus-Leidig H, Tom Dieck S, Specht D, Meyer L, Brandstätter JH (2009) Early steps in the assembly of photoreceptor ribbon synapses in the mouse retina: the involvement of precursor spheres. J Comp Neurol 512:814–824
27. Magupalli V, Schwarz K, Alpadi K, Natarajan S, Seigel GM, Schmitz F (2008) Multiple RIBEYE-RIBEYE interactions create a dynamic scaffold for the formation of synaptic ribbons. J Neurosci 28:7954–7967
28. Tom Dieck S, Altrock WD, Kessels MM, Qualmann B, Regus H, Brauner D, Fejtová A, Bracko O, Gundelfinger ED, Brandstätter JH (2005) Molecular dissection of the photoreceptor ribbon synapse: physical interaction of Bassoon and RIBEYE is essential for the assembly of the ribbon complex. J Cell Biol 168:825–836
29. Schoch S, Gundelfinger ED (2006) Molecular organization of the presynaptic active zone. Cell Tis Res 326:379–391
30. Filippi S, Motyl B, Bandera C (2008) Analysis of existing methods for 3D modelling of femurs starting from two orthogonal images and development of a script for a commercial software package. Comput Methods Programs Biomed 89:76–82
31. Ma B, Wang L, von Wasielewski R, Lindenmaier W, Dittmar KE (2008) Serial sectioning and three-dimensional reconstruction of mouse Peyer's Patch. Micron 39:967–975